# Chapter 10
# Stability and Structural Transitions in Crystal Lattices

Ekaterina Podolskaya, Artem Panchenko and Anton Krivtsov

**Abstract** The advance in nanotechnology has lead to necessity to determine strength properties of crystal structures. Stability of a structure under finite deformations is closely connected with its strength. In this work stability of plane triangular (single atomic layer of FCC and HCP) and FCC lattices under finite strain is investigated. Analysis and modeling based on discrete atomistic methods is proposed. The medium is represented by a set of particles which interact by a pair force central potential, e.g. Lennard-Jones and Morse. Direct tensor calculus is used. Dynamic stability criterion is established: frequency of elastic waves is required to be real for any real wave vector. The considered approach allows to describe structural transitions in solids on the base of stability investigation of pre-strained crystal lattices. The results of direct MD simulation do not contradict the results of the calculations.

## 10.1 Introduction

Recent advance in nanotechnology has lead to the necessity of determining mechanical properties of the minute objects. Due to being small in size such objects are often without defects, thus their strength, for instance, is close to ideal. According to [1], ideal strength is the maximum applied stress that an object can endure. Under this definition it is assumed that the object remains stable under minor strain

Ekaterina Podolskaya · Anton Krivtsov
Institute of Problems in Mechanical Engineering, Bol'shoy pr. 61, V.O., 199178 St. Petersburg & St. Petersburg State Polytechnical University, Polytechnicheskaya str. 29, 195251 St. Petersburg, Russia,
e-mail: katepodolskaya@gmail.com,akrivtsov@bk.ru

Artem Panchenko
St. Petersburg State Polytechnical University, Polytechnicheskaya str. 29, 195251 St. Petersburg, Russia,
e-mail: artemqt@yandex.ru

or stress deviations along the loading path. On the other hand, it is crucial to make sure that the object does not loose stability in terms of arbitrary minor perturbations at each strain or stress increment. If the object is described within continuum mechanics approach, analysis of ellipticity of equilibrium equations is to be carried out in order to find first failure strains [2]. However, continuum analysis is not always valid for nanoscale objects [3], because at this level influence of internal structure cannot be neglected. An ideal crystal lattice is one of the simplest models to consider within atomistic approach. The theory has been developed since works of M.Born [4], where a criterion for infinitesimal uniform deformations is established. However, it was shown in [5] that this criterion does not give adequate results if finite deformation is imposed. Moreover, further problems appear if the deformation field is inhomogeneous. For this case in continuum mechanics certain apparatus is developed, e.g. in [6]. As for atomistic approach, there are at least three ways to find the solution: homogenization (long-wave approximation etc.) and application of continuum methods, direct investigation of, e.g. corresponding spring system, and computer simulation. There has been a number of works, e.g. [7] for FCC (face-centered cubic) lattice under triaxial compression, which showed structural transition to BCC (base-centered cubic). Another series of works [8; 9] is devoted to both 2D (square lattice) and 3D (cubic lattice) structures, for which macro-(continuum) and microscopic criteria are used to obtain failure surfaces, both in case of homogeneous and inhomogeneous initial deformation. Recently, there have appeared independent investigations of graphene stability [10; 11]; its lattice should be described with more sophisticated interaction forces.

## Tensor Notation

Let us introduce the following notation concerning direct tensor calculus [2] used in this work. Vectors are denoted by lower-case letters in boldface, e.g. $\mathbf{a}$, tensors are denoted by upper-case letters in boldface with a digit specifying the rank (if the rank is not equal to two), e.g. ${}^4\mathbf{A}$, and for scalars italics is used, e.g. $A$. No special sign denotes tensor, or dyadic, product, i.e. $\mathbf{ab}$ is a dyad, $\mathbf{abc}$ is a third-rank tensor etc. For scalar product symbol $\cdot$ is used, and $\mathbf{abc}\cdots\mathbf{def} = (\mathbf{c}\cdot\mathbf{d})(\mathbf{b}\cdot\mathbf{e})(\mathbf{a}\cdot\mathbf{f})$. The notation for the divergence of vector $\mathbf{a}$ is $\nabla\cdot\mathbf{a} = \dfrac{\partial a_x}{\partial x} + \dfrac{\partial a_y}{\partial y} + \dfrac{\partial a_z}{\partial z}$, where $\nabla$ is Del operator. Gradient of vector $\mathbf{a}$ is $\nabla\mathbf{a} = \mathbf{i}_x\dfrac{\partial \mathbf{a}}{\partial x} + \mathbf{i}_y\dfrac{\partial \mathbf{a}}{\partial y} + \mathbf{i}_z\dfrac{\partial \mathbf{a}}{\partial z}$, where $\dfrac{\partial \mathbf{a}}{\partial x} = \mathbf{i}_x\dfrac{\partial a_x}{\partial x} + \mathbf{i}_y\dfrac{\partial a_y}{\partial x} + \mathbf{i}_z\dfrac{\partial a_z}{\partial x}$, $x,y,z$ are Cartesian coordinates and $\mathbf{i}_x,\mathbf{i}_y,\mathbf{i}_z$ form the corresponding basis of unit vectors. Transposed gradient of vector $\mathbf{a}$ is denoted by $\mathbf{a}\nabla$.

## 10.2 Statement of the Problem

In this work mixed approach is proposed, which includes homogenization and is similar to [10], but regards simpler objects in order to diminish computational difficulty and obtain as much as possible analytically. Firstly, only simple lattices are considered not to be distracted by sublattices-induced instabilities. Secondly, as shown in [12], central pair force interaction is applicable for stability analysis of close-packed lattices. Following the works mentioned in the previous section, we do one more simplification, which is consideration of periodic, i.e. infinite, structures, thus no surface effects will be observed. We use Lennard-Jones and Morse potentials (10.1), because they depend only on interatomic distance, they have only 2 and 3 parameters respectively and also they provide repulsion upon compression and attraction upon stretching. For 2D case triangular lattice is regarded, which is an atomic layer of FCC and HCP (hexagonal close-packed) lattices. For 3D case FCC is considered, as BCC is non-close-packed, HCP is complex and others are not so widespread as these three.

$$\Pi_M(r) = D\left[e^{-2\theta\left(\frac{r}{a}-1\right)} - 2e^{-\theta\left(\frac{r}{a}-1\right)}\right], \quad \Pi_{LJ}(r) = D\left[\left(\frac{a}{r}\right)^{12} - 2\left(\frac{a}{r}\right)^{6}\right]. \quad (10.1)$$

Parameters $D$ and $\theta$ are responsible for the potential well depth and width. Near the equilibrium position if $\theta = 6$ Morse potential is equivalent to Lennard-Jones potential with the same values of the potential well depth and equilibrium distance $a$ [13]. An important distinction of Morse potential from Lennard-Jones potential is that during the compression of the material towards $r = 0$ the interaction force remains finite, e.g. if $\theta = 6$, the repulsion force has the order of $10^6 D/a$, which is preferable for computer simulations under strong compression. In addition, rapid attenuation of exponents in Morse potential allows us to take into account the smaller number of coordination spheres.

The procedure of stability criterion derivation and explicit results for 2D case can be found in [14; 15]. The main idea is as follows. Let us consider a lattice which is infinite and without defects, not to account for boundary conditions and inhomogeneities. Using long-wave approximation [4]

$$a_k \mathbf{e}_k \approx a_k^0 \mathbf{e}_k^0 \cdot \overset{\circ}{\nabla} \mathbf{r}, \quad (10.2)$$

we can write equilibrium equations in Piola form [13]

$$\rho_0 \ddot{\mathbf{u}} = \overset{\circ}{\nabla} \cdot \mathbf{P}, \qquad \mathbf{P} = -\frac{1}{2V_0} \sum_k F_k a_k^0 \mathbf{e}_k^0 \mathbf{e}_k, \quad (10.3)$$

where $\mathbf{u}$ is displacement vector, $\mathbf{P}$ is Piola stress tensor, $a_k^0$ and $\mathbf{e}_k^0$ are the reference bond lengths and directions respectively, $F_k$, $a_k$ and $\mathbf{e}_k$ are the current forces, the current bond lengths and directions, $\rho_0$ is density and $\overset{\circ}{\nabla}$ is Del operator, both in the reference configuration, and $\overset{\circ}{\nabla} \mathbf{r}$ is transposed deformation gradient. Then,

let us find the first variation of (10.3) which takes the form of the following wave equation (10.4) for arbitrary homogeneous deformation field

$$\ddot{\mathbf{v}} = {}^4\mathbf{Q} \cdots \nabla\nabla\mathbf{v}, \tag{10.4}$$

where $\mathbf{v} = \delta\mathbf{u}$ is the first variation of the displacement vector, $\nabla$ is Del operator in current configuration. ${}^4\mathbf{Q}$ is a fourth-rank tensor that depends on the first and second derivatives of the interaction potential (current forces in bonds $F_k$ and bonds' stiffness $C_k$) as well as on the geometry of particle surroundings (10.5)

$$\begin{gathered} {}^4\mathbf{Q} = \frac{1}{\rho_0 V_0}\left(\mathbf{E}\Phi + {}^4\mathbf{B}\right), \\ \Phi = -\frac{1}{2}\sum_k F_k a_k \mathbf{e}_k\mathbf{e}_k, \quad {}^4\mathbf{B} = \frac{1}{2}\sum_k a_k^2\left(C_k + \frac{F_k}{a_k}\right)\mathbf{e}_k\mathbf{e}_k\mathbf{e}_k\mathbf{e}_k. \end{gathered} \tag{10.5}$$

Here $V_0$ is the unit cell volume in reference configuration, $\mathbf{E}$ is second rank unit tensor.

The solution of (10.4) in the wave form is

$$\mathbf{v} = \mathbf{v_0} e^{i\omega t} e^{i\mathbf{k}\cdot\mathbf{r}}, \tag{10.6}$$

where $\mathbf{k}$ is wave vector and $\omega$ is frequency. Thus, for any real wave vector frequency has to be real, i.e. $\omega^2 > 0$, so that additional minor solution $\mathbf{v}$ does not contain exponential growth. This demand leads to positive definiteness of tensor $\mathbf{D} = {}^4\mathbf{Q} \cdot \cdot \mathbf{kk}$ which looks similar to acoustic tensor that is to be positive definite to provide ellipticity [2], but it is not, because ${}^4\mathbf{Q}$ is not in fact equal to $\partial\mathbf{P}/\partial\overset{\circ}{\nabla}\mathbf{r}$. If they were equal, wave equation (10.5) would contain $\overset{\circ}{\nabla}$, not $\nabla$. Hence, instability is associated with exponential growth of the solution for perturbed state.

## 10.3 Triangular Lattice

For biaxial strain along the axes, shown in the bottom of fig.10.1, it is possible to obtain analytical solution [14; 15] in terms of components of ${}^4\mathbf{Q}$

$$\begin{gathered} Q_{11} > 0, \quad Q_{21} > 0, \quad Q_{12} > 0, \quad Q_{12} > 0, \quad B > -\sqrt{AC}, \\ A = Q_{11}Q_{21}, \quad C = Q_{12}Q_{22}, \quad 2B = Q_{11}Q_{22} + Q_{12}Q_{21} - 4Q_{44}^2, \end{gathered} \tag{10.7}$$

where two indices instead of four are used due to symmetry. All vectors and tensors introduced in the previous section are two-dimensional. In the Fig. 10.1 the stability regions of the 2D triangular lattice are plotted gray, $\varepsilon_1$ and $\varepsilon_2$ are the linear parts of the Cauchy-Green deformation tensor, the interaction is described by Morse potential (10.1) with $\theta = 6$.

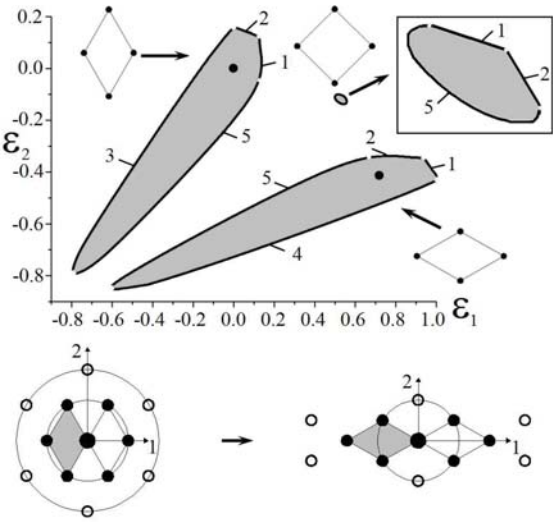


**Fig. 10.1** *Top* — stability regions of the triangular lattice in deformation space $\varepsilon_1$, $\varepsilon_2$, Morse potential with $\theta = 6$. On the boundaries positivity is lost (10.7) by: 1) $Q_{11}$, 2) $Q_{22}$, 3) $Q_{21}$, 4) $Q_{12}$, 5) $B+\sqrt{AC}$, also 1), 2), 5) by Young modulae, 3), 4) by shear modulae. *Bottom* — transition from vertical to horizontal orientation of the triangular lattice. Digits denote the coordinate axes. The unit cell is gray, the reference atom is marked by a circle, the atoms of the 1st coordination sphere — by circles of a smaller radius, the atoms of the 2nd coordination sphere — by empty circles

To check the adequacy of these results for all configurations elastic modulae are calculated using the formula for Cauchy stress tensor [13]

$$\boldsymbol{\sigma} = -\frac{1}{2V}\sum_k a_k F_k \mathbf{e_k} \mathbf{e_k}, \tag{10.8}$$

where $V = \sqrt{3}a^2/2\,(1+\varepsilon_1)\,(1+\varepsilon_2)$ is current volume of the unit cell. It turns out that the boundaries of stability regions correspond to the loss of positivity of Young modulae and shear modulae (plural is due to anisotropy). Note that during the analysis it is crucial to take at least two coordinational spheres into account, despite the cliche that if you deal with a close-packed lattice only first sphere is sufficient. As shown in the bottom of the fig.10.1, structural transition from vertical to horizontal orientation of the lattice is described within stability analysis. Consideration of larger amount of atoms does not lead to major alterations.

Analysis similar to macroscopic [8] was carried out which showed that real ellipticity condition is necessary but not sufficient (at least less sufficient, than this) for 2D case. Nearly the same results were achieved with Lennard-Jones potential. The main difference is that this interaction provides stability during compression right up to deformations arbitrarily close to point $\varepsilon_1 = \varepsilon_2 = -1$. This effect contradicts the results for FCC lattice, achieved in [7].

In addition, an MD (molecular dynamical) simulation is carried out. The simulation technique is described in [13]. For a series of deformed configurations we perform the following computational experiment. As the initial condition, we construct a triangular lattice in the deformed state with periodic boundary conditions, that account for infinite lattice. The interaction is described by means of the same Morse potential. The initial kinetic energy of the particles does not exceed $0.0002D$.

The system evolution is described by the solution of the Cauchy problem for the set of ordinary differential equations

$$m\ddot{\mathbf{r}}_k = \sum_{n=1}^{N} F\left(|\mathbf{r}_k - \mathbf{r}_n|\right) \frac{\mathbf{r}_k - \mathbf{r}_n}{|\mathbf{r}_k - \mathbf{r}_n|}, \tag{10.9}$$

where $N$ is the number of particles, $m$ is the particle mass, and $\mathbf{r}_k$ is the radius-vector of the $k$th particle. If further we observe oscillations of the kinetic energy around a certain value not exceeding $0.0002D$, we conclude that this configuration is stable. If we observe a sudden growth of the kinetic energy, the deformed configuration is considered unstable. A very good agreement with analytical results is observed. However, in MD one can only distinguish between 100% unstable cases and cases, when instability has not been reached. In addition, the more accurate regions' borders are needed, the longer lasts the calculation. Stable regions endured $3 \cdot 10^5$ integration steps, whereas others — not more than $10^5$ steps, excluding border zones. MD experiment shows, what exactly happens after stability is lost: either the material may become liquid, or a crack may appear (see Fig. 10.2).

Similar results were achieved for deformation including shear [15], described by deformation gradient with the following affine transformation

$$\mathbf{r} \overset{\circ}{\nabla}\sim \begin{pmatrix} 1+\varepsilon_1 & \operatorname{tg}\varphi_{21} \\ 0 & 1+\varepsilon_2 \end{pmatrix}. \tag{10.10}$$

There are only three elements in the tensor (10.10) in order to exclude solid-body rotations from consideration.

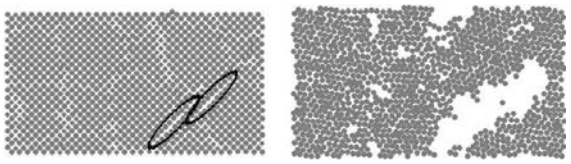

**Fig. 10.2** Unstable configuration after $10^5$ (left) and $3 \cdot 10^5$ (right) integration steps. Black ovals mark "crack" initiation zones

## 10.4 FCC Lattice

In 3D case more or less analytical results can be obtained only for diagonal affine transformation, whose eigenvectors coincide with axes of cubic symmetry, and are partially presented in [16]

$$\mathbf{r} \overset{\circ}{\nabla}\sim \begin{pmatrix} 1+\varepsilon_1 & 0 & 0 \\ 0 & 1+\varepsilon_2 & 0 \\ 0 & 0 & 1+\varepsilon_3 \end{pmatrix}. \tag{10.11}$$

We use Morse potential, because Lennard-Jones allows infinite compression which contradicts [7]. Three coordinational spheres are considered, because the distance between the reference atom and the atoms of the third sphere is the same as the distance between the reference atom and the atoms of the second sphere in triangular lattice. Positive definiteness of tensor **D**, i.e. stability, is ensured if

$$D_{11} > 0, \quad D_{11}D_{22} - D_{12}D_{21} > 0, \quad \det D > 0. \tag{10.12}$$

Left parts of (10.12) are homogeneous functions of wave vector components of degree two, four and six respectively, and contain only even degrees. Inequalities (10.12) should hold for any real wave vector. In this case we cannot fully exclude wave vector components from consideration and obtain stability criterion only in terms of components of ${}^4\mathbf{Q}$. However, first of all, we have a necessary condition of $I_1$ positive definiteness. Moreover, we can write a series of sufficient conditions by extracting quadratic forms from left parts of inequalities (10.12). Then, for those cases, when only necessary condition shows stability, Monte-Carlo method is used.

**Proposition 10.1.** *Suppose a homogeneous polynomial $P(x,y,z)$ is positive for $x > 0$, $y > 0$, $z > 0$. Then substitution $z = 1 - x - y$ leads to positivity of $\tilde{P}(x,y)$ for $x > 0, y > 0, x + y < 1$.*

This proposition is used to speed up the Monte-Carlo calculations, as inequalities (10.12) contain only even degrees of wave vector components. In the Fig. 10.3 we can observe a major stable area, which resembles 2D case, and three additional zones, which make the region non-convex. After calculating coordinational num-

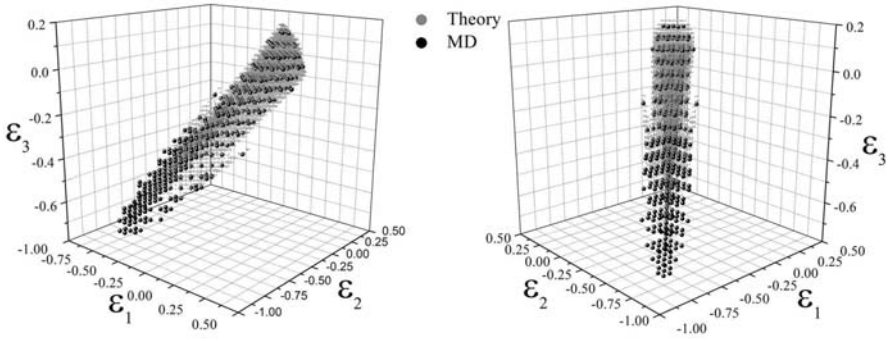


**Fig. 10.3** Stability region of FCC lattice in deformation space $\varepsilon_1$, $\varepsilon_2$, $\varepsilon_3$, Morse potential with $\theta = 6$, three coordinational spheres. Grey points — theoretical result, black points — MD result

bers of deformed lattices that form additional zones, we can conclude that they are compressed BCC lattices.

Using Bain method [17] we can write an affine transformation from equilibrium FCC to equilibrium BCC (see Fig. 10.4a)

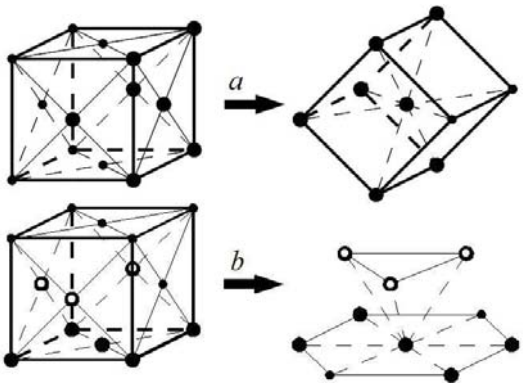


**Fig. 10.4** Transitions: *a* from FCC (left) to BCC (right), *b* from FCC to FCC

$$\varepsilon_1 = \varepsilon_2 = \frac{2}{\sqrt{3}}\frac{\rho_{BCC}}{\rho_{FCC}} - 1, \quad \varepsilon_3 = \frac{\sqrt{2}}{\sqrt{3}}\frac{\rho_{BCC}}{\rho_{FCC}} - 1 \tag{10.13}$$

Here we need to take into account so-called "bond compression" which occurs when more than one coordinational sphere is regarded: equilibrium distance $\rho$ between neighboring atoms is smaller than that of the potential.

Due to topological differences between FCC and BCC, two spheres of FCC contain 18 atoms, and two spheres of BCC have only 12. Hence, if initial FCC has equilibrium with, e.g. two spheres, stress tensor for obtained BCC will be non-zero. This problem can be solved by cut-off interaction, e.g. [13]

$$\tilde{F}(r) = k(r)F(r), \tag{10.14}$$

where $k(r)$ is shape function

$$k(r) = \begin{cases} 1, & r \le b, \\ \left(1 - \left(\dfrac{r^2 - b^2}{a_{cut}^2 - b^2}\right)^2\right)^2, & b < r \le a_{cut}, \\ 0, & r > a_{cut} \end{cases} \tag{10.15}$$

Here $a_{cut}$ is the cut-off distance, $b$ is the critical bond length, i.e. $F'(b) = 0$.

Now, if we plot stress-strain diagram for cut-off smooth potential (10.14) on the base of Morse potential, we will see, that equilibrium BCC may be gained from equilibrium FCC by simple uniaxial compression, e.g. $\sigma_1 \neq 0, \sigma_2 = \sigma_3 = 0$ (see Fig. 10.5 for $\theta = 4$). Due to symmetry there are all in all three equilibrium BCC lattices. Moreover, equilibrium BCC is unstable if $\theta = 6$, and Lennard-Jones does not describe BCC-zones at all, and these results correspond to [7; 18]. If we make the potential well wider, BCC will be stable, though more spheres should be accounted for (see Fig. 10.5). Unfortunately, BCC zones do not separate from FCC, leaving the possibility of stable FCC-BCC transition. On the other hand, stability region

is non-convex (Fig. 10.5), so "Bain deformation" [17], which is accomplished by strain, not stress, will provide an unstable zone between FCC and BCC equilibria.

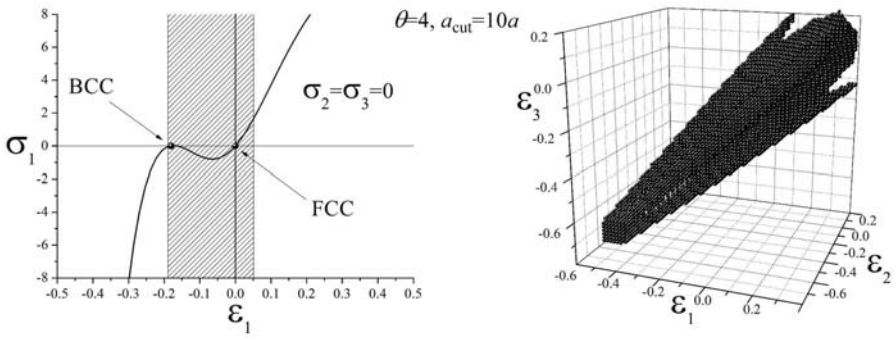


**Fig. 10.5** *Left* — uniaxial loading, hatching indicate stability region. *Right* — stability region of FCC lattice in deformation space $\varepsilon_1$, $\varepsilon_2$, $\varepsilon_3$, smooth cut-off Morse potential with $\theta = 4$, $a_{cut} = 10a$.

The next step is to include shear into consideration. To get rid of as many solid-body rotations as possible, the following transformation is used

$$\mathbf{r} \overset{\circ}{\nabla} \sim \begin{pmatrix} 1+\varepsilon_1 & \mathrm{tg}\varphi_{21} & 0 \\ 0 & 1+\varepsilon_2 & \mathrm{tg}\varphi_{32} \\ \mathrm{tg}\varphi_{13} & 0 & 1+\varepsilon_3 \end{pmatrix}. \tag{10.16}$$

Using Bain method [17] again, we can find six FCC lattices of the following origin (see Fig. 10.4b)

$$\varepsilon_1 = \frac{\sqrt{3}}{\sqrt{2}} - 1, \quad \varepsilon_2 = \frac{2}{\sqrt{3}} - 1, \quad \varepsilon_3 = \frac{1}{\sqrt{2}} - 1, \quad \mathrm{tg}\varphi_{21} = \pm\frac{1}{\sqrt{6}}, \tag{10.17}$$

which may look as if we just turned one of the axis of cubic symmetry to [1,1,1] axis.

MD simulation was carried out for triaxial strain and showed again a good agreement except for the "tail" zone (see Fig. 10.3), which is due to different number of coordinational spheres considered: the more atoms, the longer the "tail", i.e. maximum compression for uncut Morse potential varies from 60% for three coordinational spheres to 75%. As stated before, Lennard-Jones potential is not suitable for MD under high compression, because of infinite forces upon infinite compression.

In addition, analysis for FCC in different axes is performed, so that triangular lattice plane problem could be accounted for. Again, two major regions in triaxial strain space are obtained, but their cross-sections differ from 2D results, since in 2D study only 2D wave vectors are considered (see Fig. 10.6). Thus, we can conclude,

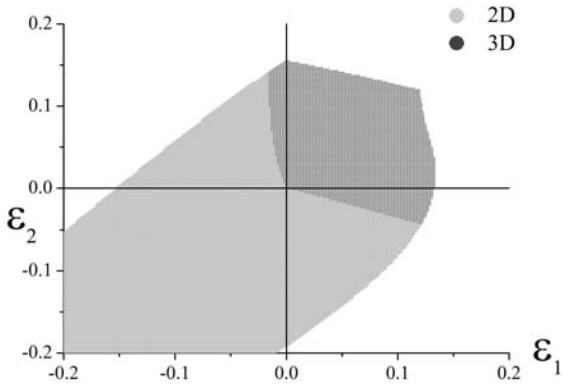


**Fig. 10.6** Stability region of triangular lattice for 2D (light gray) and 3D (dark gray) wave vector.

that vast stability region at compression vanishes, if minor perturbations in third direction occur.

## 10.5 Concluding Remarks

In this work stability analysis of infinite triangular and FCC lattices without defects is carried out. Instability is associated with exponential growth of the solution for perturbed state. The considered approach allows to describe structural transitions on the base of stability investigation of pre-strained crystal lattices (see Figs. 10.1 and 10.4). FCC-BCC transition is examined, and several conclusions can be drawn. Due to topological differences between the lattices smooth cut-off interaction force is to be used. Lennard-Jones potential does not describe BCC zones, whereas Morse potential is applicable if the potential well is wide enough, but this demand leads to consideration of additional coordinational spheres. Equilibrium BCC may be obtained from equilibrium FCC by simple uniaxial compression, though the whole loading path is stable, as BCC stability zones do not separate from FCC one. On the other hand, stability region is non-convex (fig.10.5), so "Bain deformation" [17], which is accomplished by strain will provide an unstable zone between FCC and BCC equilibria. Furthermore, it is shown that stability region for triangular lattice diminishes, especially in compression zone, if 3D perturbations are imposed (Fig. 10.6). MD simulation is carried out for verification of theoretical results, and they prove to be in good agreement.

**Acknowledgements** Authors are deeply grateful to prof. D.A. Indeitsev, prof. E.A. Ivanova and prof. N.F. Morozov for useful discussions. This work was supported by grants of St. Petersburg Government (acts No.72, 25.10.2011 and No.80, 01.11.2011) and RFBR (No.11-01-00809-a, No.12-01-31297 mol-a).

## References


1. Macmillan, N.H.: The ideal strength of solids. In: Latanision, R., Pickens, J.R. (eds.) Atomistic of Fracture, pp. 95–164. Plenum Press, New York (1983)
2. Lurie, A.I.: Nonlinear Theory of Elasticity. North-Holland, Amsterdam (1990)
3. Krivtsov, A.M., Morozov, N.F.: On mechanical characteristics of nanocrystals. Phys. Solid State **44**(12), 2260–2265 (2002)
4. Born, M., Huang, K.: Dynamical Theory of Crystal Lattices. Clarendon, Oxford (1954)
5. Wang,J., Li, J., Yip, S., Phillpot, S., Wolf, D.: Mechanical instabilities of homogeneous crystals. Phys. Rev. **52**(17B), 12627–12635 (1995)
6. Fu, Y.B., Ogden, R.W.: Nonlinear stability analysis of pre-stressed elastic bodies. Continuum Mech. Thermodyn. **11**, 141–172 (1999)
7. Milstein, F., Rasky, D.: Theoretical study of shear-modulus instabilities in the alkali metals under hydrostatic pressure. Phys. Rev. **54**(10), 7016–7025 (1996)
8. Schraad, M., Triantafyllidis, N.: Effects of Scale Size on Media with Periodic and Nearly Periodic Microstructures – II Failure Mechanisms. Journal Appl. Mech. **64**, 762–771 (1997)
9. Elliott, R.S., Shaw J.A., Triantafyllidis, N.: Stability of pressure-dependent, thermally-induced displacive transformations in bi-atomic crystals. International Journal of Solids and Structures. **39**, 3845–3856 (2002)
10. Tovstik, P.E., Tovstik, T.P.: On the 2D graphite layer model. Vestnik of the St. Petersburg University: Mathematics, **3**, 134–143 (2009) [in Russian]
11. Dmitriev, S.V., Baimova, Yu.A., Savin, A.V., Kivshar', Yu.S.: Stability range for a flat graphene sheet subjected to in-plane deformation. JETP Letters. **93**(10), 571–576 (2011)
12. Wallace, D.C., Patrick, J.L.: Stability of crystal lattices. Phys. Rev. **137**(1A), 152–160 (1965)
13. Krivtsov, A.M.: Deformation and Fracture of Solids with Microstructure. Fizmatlit, Moscow (2007) [In Russian]
14. Podolskaya, E.A., Panchenko, A.Yu., Krivtsov, A.M.: Stability of 2D triangular lattice under finite biaxial strain. Nanosystems: Phys., Chem., Math. **2**(2), 84–90 (2011)
15. Podolskaya, E.A., Panchenko, A.Yu., Krivtsov, A.M., Tkachev, P.V.: Stability of ideal infinite 2D crystal lattice. Doklady Physics **57**(2), 92–95 (2012)
16. Podolskaya, E.A., Krivtsov, A.M., Panchenko, A.Yu.: Investigation of stability and structural transition in FCC lattice under finite strain. Vestnik of the St. Petersburg University: Mathematics [in press]
17. Bain, E. C.: The nature of martensite. Trans. Amer. Inst. Min. Metall. Eng. **70**, 25–46 (1924)
18. Berinskii, I.E. et.al: Theoretical Mechanics. Elastic Properties of Monoatomic and Diatomic Crystals. Ed. by A. M. Krivtsov. St. Petersburg State Polytechnical University, St. Petersburg (2009) [in Russian].